Jahn-Teller effect problems via ultrasonic experiments. Application to the impurity crystal CdSe:Cr

IOP Conf. Series: Journal of Physics: Conf. Series **1148** (2018) 012008 doi:10.1088/1742-6596/1148/1/012008

Jahn-Teller effect problems via ultrasonic experiments. Application to the impurity crystal CdSe:Cr

N S Averkiev[1], I B Bersuker[2], V V Gudkov[3,8], I V Zhevstovskikh[3,4], M N Sarychev[3], S Zherlitsyn[5], S Yasin[5,9], Yu V Korostelin[6] and V T Surikov[7]

[1] A F Ioffe Institute, St. Petersburg, 194021, Russia
[2] University of Texas at Austin, Institute for Theoretical Chemistry, Austin, TX 78712, USA
[3] Institute of Physics and Technology, Ural Federal University, Ekaterinburg, 620002, Russia
[4] M N Miheev Institute of Metal Physics, Ural Branch of Russian Academy of Sciences, Ekaterinburg, 620137, Russia
[5] Hochfeld-Magnetlabor Dresden (HLD-EMFL), Helmholtz-Zentrum Dresden-Rossendorf, 01328 Dresden, Germany
[6] P N Lebedev Physical Institute of Russian Academy of Sciences, Moscow, 119991, Russia
[7] Institute of Solid State Chemistry, Ural Branch of Russian Academy of Sciences, Ekaterinburg, 620990, Russia

Abstract. Based on the data analysis of ultrasonic experiments, a novel approach has been developed to explore Jahn-Teller effect (JTE) problems in non-cubic crystals with JT centers without involving additional experimental data beyond the information about the electronic term and crystal symmetry. Distinguished from cubic crystals, the axis of symmetry of the bulk non-cubic crystal do not necessarily coincide with those of the local impurity center, thus complicating the relation between the distortions produced by the ultrasound wave and the JTE active modes. We analysed the problem with corresponding calculations for the wurtzite-type hexagonal crystal CdSe:Cr^{2+}, in which the chromium ion substitutes the cadmium one in the tetrahedral environment, resulting in its electronic ground state $^5T_2\left(e^2t^2\right)$. Experimental investigation of this system by ultrasound at frequencies of 28 -105 MHz in the temperature range of 4-180 K, yields a peak in the attenuation of the ultrasound below 40 K for the normal modes related to the c_{11}, c_{44}, c_{55}, and c_{66} elastic moduli. The peak has been interpreted as the manifestation of the JTE, similar to the one, observed in cubic crystals doped with 3*d* ions. However, no anomalies of attenuation have been detected for the mode related to the c_{33} elastic modulus, in contradiction to the theoretical

[8] Email: gudkov@imp.uran.ru, v.vgudkov@urfu.ru
[9] Present address: American University of the Middle East (AUM), College of Engineering and Technology, Egaila 54200, Kuwait

predictions based on the previous method, worked out for cubic crystals. In the new method we obtained direct relations between the deformations, related to the crystal moduli, and the local JT modes, calculated the partition functions for each of the three possible JTE problems for systems with an electronic T term, $T\otimes e$, $T\otimes t_2$, and $T\otimes(e+t_2)$, and revealed how these deformations alter the vibronic energy levels responsible for the relaxations in the JT centers. It emerged that in the wurtzite crystal under consideration, only in the $T\otimes e$ problem the deformation related to the elastic moduli c_{33} displaces all the vibronic energy level uniformly, without relaxation possibilities, thus supporting the new method and explaining the experimental observations.

1. Introduction

In continuation of our previous studies showing that ultrasonic experiments are very instrumental in determining the parameters of the adiabatic potential energy surfaces (APES) of Jahn-Teller effect (JTE) centers in crystals[1] and their changes in magnetic fields,[2,3] we worked out a more general approach to the problem, that allows us to reveal the type of the JTE problem without involving other experimental data beyond the electronic term and crystal symmetry. Our former approach to the problem has been related to *cubic crystals* doped with 3d ions, sphalerites (see, e.g., reference [2] and references therein) and fluorites.[4,5] In such crystals, the impurity ion occurs in tetrahedral (sphalerite) or cubic (fluorite) coordination, and the ultrasonic wave propagating along the principal crystallographic axis (ultrasonic normal mode) produces distortions with symmetry properties corresponding to one of the local vibronic coupling modes, active in the JTE.[2] This, in turn, violates the equivalency between the minima of the APES produced by the JTE, shifting their energy levels differently (up or down) in different minima, thus destroying the thermal equilibrium between them. The relaxation to the equilibrium state with equally populated minima of the APES is the source of dissipation of the wave energy, leading to additional ultrasound attenuation and dispersion, which is seen also as a variation in phase velocity. Hence the anomalies in the attenuation and dispersion of the normal mode ultrasound propagation in these cases indicate directly the JTE active modes (the distortion symmetry).

In a cubic crystal, the normal mode related to the $(c_{11}-c_{12})/2$ modulus produces tetragonal distortions of the JTE center described by vibronic *e*-type modes, while the mode related to the c_{44} modulus produces trigonal distortions, *t*-type vibronic modes. This approach allowed us to show that in ZnSe:Cr^{2+} the $T\otimes e$ JTE problem takes place, while the $T\otimes(e+t_2)$ problem with orthorhombic global minima of the APES is realized in SrF_2:Cr^{2+},[4,5] as well as in ZnSe with the JT centers formed by zinc vacancies.[6]

However, the described above approach to the interpretation of the experimental data on ultrasound attenuation and phase velocity, worked out for cubic crystals with JTE impurities, is not directly applicable to crystals with non-cubic symmetries. For them, a reconsideration of the problem in a new, more elaborate approach is necessary, as shown in this paper. As a working example, we addressed the problem of a wurtzite crystal, CdSe:Cr^{2+}. In contrast to a cubic crystal which has three independent components of the elastic moduli tensor (c_{11}, c_{12}, and c_{44}), hexagonal crystals possesses five independent components ($c_{11}, c_{12}, c_{13}, c_{33}$, and c_{44}). We have studied the modes related to c_{11}, c_{33}, c_{44}, c_{55}, and $c_{66}=(c_{11}-c_{12})/2$. Conventionally, $c_{55}=c_{44}$, but CdSe is a piezoelectric crystal, and c_{55} is the piezoelectric modulus that differs from the non-piezoelectric c_{44}. Anomalies in the

ultrasound attenuation, typical for the relaxation process, have been found in CdSe:Cr^{2+} for all the modes except those related to c_{33}. In disagreement with these findings, the application of the former approach, worked out for classical cubic crystals, yields incomprehensible results, indicating the presence of both the *e*- and *t*-type JT active vibronic modes with relaxation anomalies for all the ultrasonic normal modes, without exceptions.

To clarify this controversy we performed a thorough analysis of the distortions of the JT centers produced by the ultrasonic wave in the wurtzite-type crystal in relation to their local displacements along the vibronic coupling modes, and calculated the partition functions for each of the three possible JTE problems for systems with an electronic T term, $T\otimes e$, $T\otimes t_2$, and $T\otimes(e+t_2)$. We found that the ultrasonic modes that produce tetragonal or trigonal distortions of the unit cell of the non-cubic crystal do not produce the same symmetry distortions of the tetrahedral JT center. Note that while the crystal as a whole is non-cubic, the local symmetry in the JT impurity center is cubic-tetrahedral, and the controversy emerges due to the differences in the symmetry axis and deformation moduli of the bulk crystal and the symmetry of the vibronic coupling modes in local JT center. Notably, by applying the new approach we found that the mode related to the crystal c_{33} modulus in the case of the $T\otimes e$ JTE problem shifts the energy levels in the three equivalent minima of the APES *identically*, thus excluding any relaxation process related to this distortion. Such situations do not occur in systems with $T\otimes t_2$ or $T\otimes(e+t_2)$ JT problems.

2. Experiment

2.1. Crystal properties

The sample of the CdSe crystal doped with Cr^{2+} ions was cut off a single crystal grown in P. N. Lebedev Physical Institute of the Russian Academy of Sciences. The seeded physical vapor transport method reported in reference[7] was used with the CrSe source for doping. Concentration of the impurities was determined at the Institute of Solid State Chemistry, Ural Branch of the Russian Academy of Sciences, by the inductive coupled plasma mass spectrometer (ICP-MS), using the quadrupole based instrument ELAN 9000 (Perkin-Elmer SCIEX) with standard operating and acquisition parameters. Chromium concentration proved to be $n=(1.41\pm0.07)\times10^{18}$ cm^{-3}, significantly exceeding the concentration of other 3*d* impurities (Co, Cu, Mn, Ni, Ti, V).

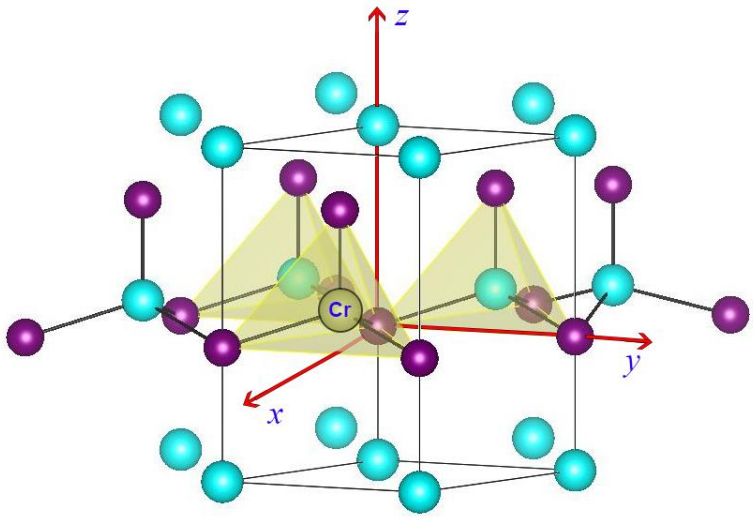

Figure 1. The tetrahedral JT center $CrSe_4$ in the CdSe matrix of the hexagonal wurtzite crystal.

The chromium dopants replace cadmium in the wurtzite lattice sites, and are surrounded by four selenium ions in the corners of a regular tetrahedron (figure 1). The ^5D term of the free Cr^{2+} ion is split by the tetrahedral crystal field into the ground orbital triplet $^5T_2$ and excited doublet ^5E. Due to the JTE, the tetrahedral coordination of the Cr^{2+} ion in degenerate $^5T_2$ state is unstable with respect to twofold e and threefold t_2 type displacements of the environment. In the linear approximation of the vibronic interaction, the dominant coupling with one of these two types of displacements results in either tetragonal or trigonal minima of the APES. With the quadratic terms included, orthorhombic minima involving both trigonal and tetragonal local modes become possible. The terminology "trigonal" and "tetragonal" is used by analogy with the symmetry properties of the octahedral and cubic coordination of the JT center; with regard to tetrahedral coordination these terms are related to distortions of the cube associated with the tetrahedron, as shown in figure 2. The tetrahedron is formed from the cube by deleting half of the ions positioned at its corners (1, 3, 5', 5"), while the other four ions (2', 2", 3, 6) remain put. In this scheme, the tetragonal distortions correspond to elongation (shortening) of one of the cube edges, the trigonal distortions correspond to elongation (shortening) of one of the cube diagonals, and the orthorhombic distortions correspond to elongation (shortening) of the cube face diagonals.

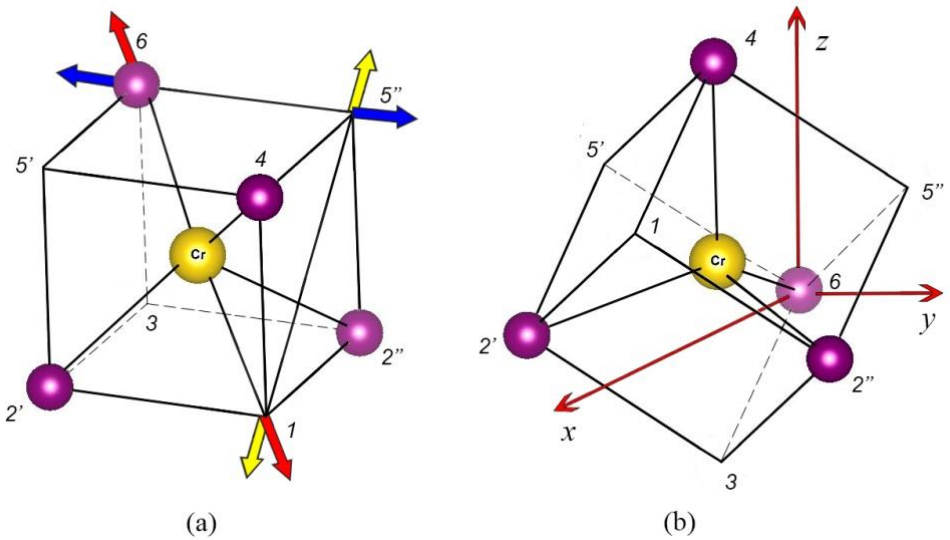

Figure 2. (a) Schematic cubic geometry associated with the JT tetrahedron. Principal deformations of the lattice are equivalent to the changes in the main cubic dimensions: cubic edge length in tetragonal deformation (blue arrows), cubic diagonal in trigonal distortion (red arrows), and face diagonal in orthorhombic deformation (yellow arrows). (b) The position of the cube is inclined with respect to the main axes of the CdSe matrix.

2.2. Ultrasonic experiment description

Ultrasonic experiments were carried out at Ural Federal University and at Dresden High Magnetic field Laboratory with the help of a setups operating as a frequency variable bridge.[8,9] The ultrasonic waves were generated and registered by a $LiNbO_3$ piezoelectric transducers at frequencies of 28-105 MHz. The studied ultrasound wave modes are listed in table 1.

2.3. Ultrasound attenuation

The attenuation coefficient of the ultrasonic mode equals the imaginary part of its negative complex wave number $\mathbf{k}$, which is defined by the corresponding component of the dynamic (i.e., frequency dependent) elastic moduli tensor $\mathbf{c}$ (also complex). The spatial ($\mathbf{r}$) and time (t)

Table 1. Properties of the studied ultrasonic modes.

Elastic modulus	Wave propagation axis	Direction of displacements	Polarization type (symmetry)	Piezo-activity
c_{11}	[100], [10$\bar{1}$0]	[100], [10$\bar{1}$0]	longitudinal	non-piezo-active
c_{33}	[001], [0001]	[001], [0001]	longitudinal	piezo-active
c_{44}	[001], [0001]	[100], [10$\bar{1}$0]	shear (T)	non-piezo-active
c_{55}	[100], [10$\bar{1}$0]	[001], [0001]	shear (T)	piezo-active
c_{66}	[100], [10$\bar{1}$0]	[010], [$\bar{1}$2$\bar{1}$0]	shear (E)	non-piezo-active

dependence of the variables, associated with the ultrasonic wave, are introduced as $\exp\left[\mathrm{i}\left(\omega t-\mathbf{k}\cdot\mathbf{r}\right)\right]$, and the component of the wave vector, corresponding to the wave propagation, is defined as $k=\omega/v-\mathrm{i}\alpha$ (here ω is the frequency of the wave, and v is its phase velocity). Since the elastic moduli are derivatives of the Helmholtz free energy (or internal energy), they comprise contributions of all the subsystems of the studied object. Consequently, attenuation of the waves caused by relaxation in the JT subsystem can be written as follows (see, e.g., reference[2]):

$$\alpha_i=-\frac{1}{2}k_{0i}\frac{\left(c_{JT}^{T}\right)_{ii}}{\left(c_0\right)_{ii}}\frac{\omega\tau}{1+\left(\omega\tau\right)^2}, \tag{1}$$

where $\left(c_{JT}^{T}\right)_{ii}$ is the isothermal contribution of the JT subsystem to the total elastic modulus c_{ii} (table 1), τ is the relaxation time, and the subscript 0 identifies the variables defined at the reference temperature $T=T_0$.

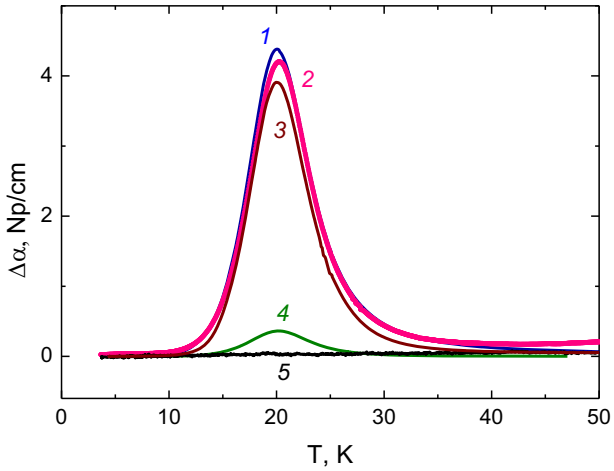

Figure 3. Temperature dependence of attenuation of the ultrasound modes related to the moduli c_{55} (curve 1, $\omega/2\pi=55.3$ MHz), c_{66} (curve 2, $\omega/2\pi=52.9$ MHz), c_{44} (curve 3, $\omega/2\pi=55.2$ Hz), c_{11} (curve 4, $\omega/2\pi=55.3$ MHz), and c_{33} (curve 5, $\omega/2\pi=55.6$ MHz; no anomalies for this modulus), $\Delta\alpha=\alpha\left(T\right)-\alpha\left(T_0\right)$, $T_0=1.5$ K.

Figure 3 shows the anomalies in the attenuation we found for the ultrasonic normal modes related to the c_{11}, c_{44}, c_{55}, and c_{66} elastic moduli below 40 K. No anomalies of attenuation have been found for the mode related to the c_{33} elastic modulus. The peak of attenuation shown in figure 3 is reduced and shifted towards lower temperatures by decreasing the ultrasound frequency, which t is typical for anomalies of relaxation origin. The relaxation origin of these anomalies are justified in the Appendix.

3. Relations between Jahn-Teller distortions and elastic moduli in wurtzite crystals

Using the wurtzite crystal under consideration as an example, we show how the problem of interpretation of experimental data on ultrasound attenuation and phase-velocity change in non-cubic crystals with JTE impurities can be solved by analyzing the influence of the distortion produced by the ultrasonic wave on the energy levels of the JT center $CrSe_4$ in CdSe matrix. For this purpose, we first identify the coordinates of the cube, associated with the tetrahedron (figure 2). Then we consider the variations of the cube's edges, cube's diagonals, and face diagonals caused by the distortions produces by the normal modes, and with these data we derive the expressions for shift of the energy levels of the system, assuming either $T \otimes e$, or $T \otimes t_2$, or $T \otimes (e + t_2)$ JTE problems. Finally, we analyze the possible relaxations in all these cases.

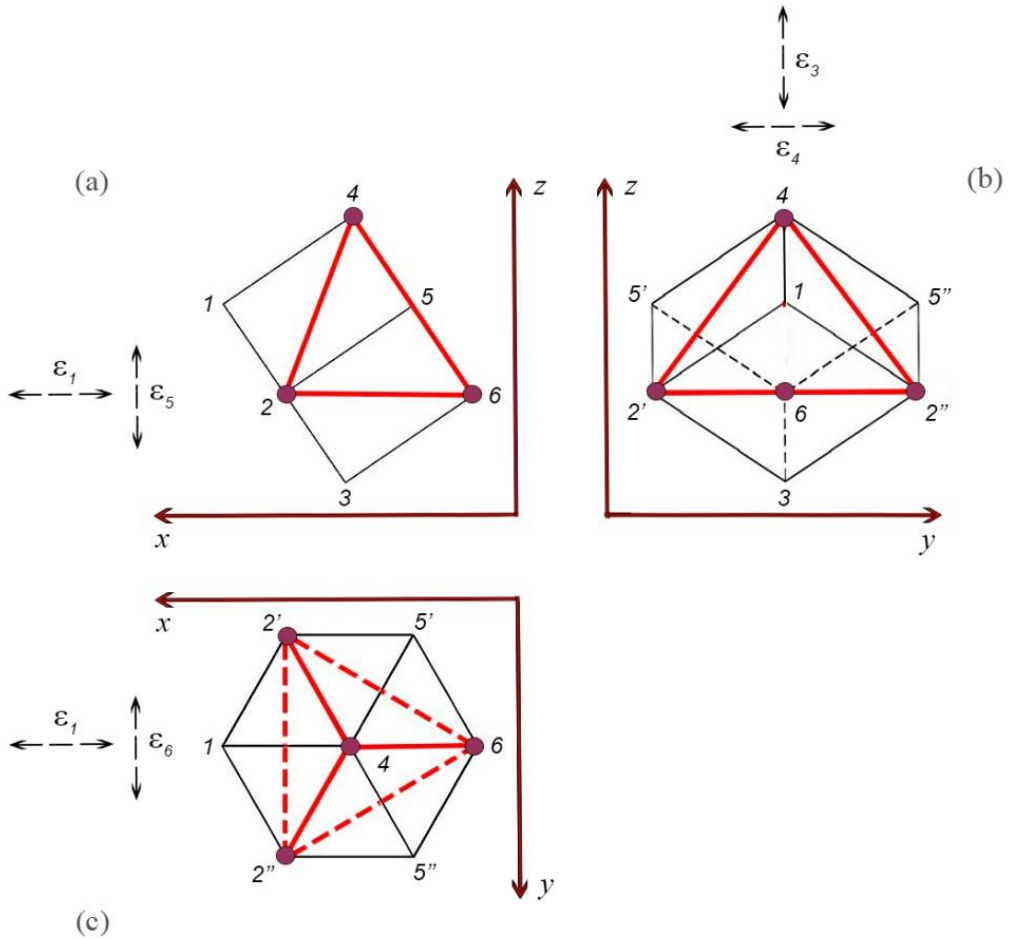

Figure 4. Conventional projection views of the cube (dark lines) associated with the JT tetrahedron (red lines) with indication of the directions of the deformations ε (shown by double arrows): (a) in view from the negative y axis, (b) in view from the negative x axis, and (c) in the top view (from the negative z axis).

3.1. The cube associated with the tetrahedron

The positions of the cube corners in Cartesian coordinates with the origin in the point 6 of figure 2 (see also figure 4) are as follows:

$$\mathbf{r}_6=(0,0,0),\ \mathbf{r}_1=\left(\frac{2}{\sqrt{3}}a,0,\frac{a}{\sqrt{6}}\right),\ \mathbf{r}_{2'}=\left(a\frac{\sqrt{3}}{2},-\frac{a}{2},0\right),\ \mathbf{r}_{2''}=\left(a\frac{\sqrt{3}}{2},\frac{a}{2},0\right),$$
$$\mathbf{r}_3=\left(\frac{a}{\sqrt{3}},0,-\frac{a}{\sqrt{6}}\right),\ \mathbf{r}_4=\left(\frac{a}{\sqrt{3}},0,\sqrt{\frac{2}{3}}a\right),\ \mathbf{r}_{5'}=\left(\frac{a}{2\sqrt{3}},-\frac{a}{2},\frac{a}{\sqrt{6}}\right),\ \mathbf{r}_{5''}=\left(\frac{a}{2\sqrt{3}},\frac{a}{2},\frac{a}{\sqrt{6}}\right),\qquad(2)$$

where a is the lattice parameter, being also the magnitude of the face diagonal. We consider the following deformations ε produced by u_x, u_y, u_z displacements in the ultrasonic wave:

$$\varepsilon_1=\varepsilon_{11}=\left[\frac{1}{2}\left(2\frac{\partial u_x}{\partial x}\right)\right]=\frac{\partial u_x}{\partial x},\ \varepsilon_3=\varepsilon_{33}=\frac{1}{2}\left(2\frac{\partial u_z}{\partial z}\right)=\frac{\partial u_z}{\partial z},$$
$$\varepsilon_4=2\varepsilon_{23}=2\left[\frac{1}{2}\left(\frac{\partial u_y}{\partial z}+\frac{\partial u_z}{\partial y}\right)\right]=\frac{\partial u_y}{\partial z},\ \varepsilon_5=2\varepsilon_{31}=2\left[\frac{1}{2}\left(\frac{\partial u_z}{\partial x}+\frac{\partial u_x}{\partial z}\right)\right]=\frac{\partial u_z}{\partial x}$$
$$\varepsilon_6=2\varepsilon_{21}=2\left[\frac{1}{2}\left(\frac{\partial u_y}{\partial x}+\frac{\partial u_x}{\partial y}\right)\right]=\frac{\partial u_y}{\partial x}.\qquad(3)$$

3.2. Variation of the corners' coordinates

Deformation of ε_1 type shifts the coordinates in the x direction: $r_x=(r_x)_0+(r_x)_0\cdot\varepsilon_1$:

$$\mathbf{r}_1=\left(\frac{2}{\sqrt{3}}a(1+\varepsilon_1),0,\frac{a}{\sqrt{6}}\right),\ \mathbf{r}_{2'}=\left(a\frac{\sqrt{3}}{2}(1+\varepsilon_1),-\frac{a}{2},0\right),\ \mathbf{r}_{2''}=\left(a\frac{\sqrt{3}}{2}(1+\varepsilon_1),\frac{a}{2},0\right)$$
$$\mathbf{r}_3=\left(\frac{a}{\sqrt{3}}(1+\varepsilon_1),0,-\frac{a}{\sqrt{6}}\right),\ \mathbf{r}_4=\left(\frac{a}{\sqrt{3}}(1+\varepsilon_1),0,\sqrt{\frac{2}{3}}a\right),\mathbf{r}_{5'}=\left(\frac{a}{2\sqrt{3}}(1+\varepsilon_1),-\frac{a}{2},\frac{a}{\sqrt{6}}\right),$$
$$\mathbf{r}_{5''}=\left(\frac{a}{2\sqrt{3}}(1+\varepsilon_1),\frac{a}{2},\frac{a}{\sqrt{6}}\right)\qquad(4)$$

Deformation of ε_3 type shifts the coordinates in the z direction: $r_z=(r_z)_0+(r_z)_0\cdot\varepsilon_3$:

$$\mathbf{r}_1=\left(\frac{2}{\sqrt{3}}a,0,\frac{a}{\sqrt{6}}(1+\varepsilon_3)\right),\ \mathbf{r}_{2'}=\left(\frac{\sqrt{3}}{2}a,-\frac{a}{2},0\right),\ \mathbf{r}_{2''}=\left(\frac{\sqrt{3}}{2}a,+\frac{a}{2},0\right),$$
$$\mathbf{r}_3=\left(\frac{a}{\sqrt{3}},0,-\frac{a}{\sqrt{6}}(1+\varepsilon_5)\right),\ \mathbf{r}_4=\left(\frac{a}{\sqrt{3}},0,\sqrt{\frac{2}{3}}a(1+\varepsilon_3)\right),\ \mathbf{r}_{5'}=\left(\frac{a}{2\sqrt{3}},-\frac{a}{2},\frac{a}{\sqrt{6}}(1+\varepsilon_3)\right)$$
$$\mathbf{r}_{5'}=\left(\frac{a}{2\sqrt{3}},\frac{a}{2},\frac{a}{\sqrt{6}}(1+\varepsilon_3)\right).\qquad(5)$$

Deformation of ε_4 type shifts the coordinates in the y direction: $r_y = \left(r_y\right)_0 + \left(r_z\right)_0 \cdot \varepsilon_4$:

$$\mathbf{r}_1 = \left(\frac{2}{\sqrt{3}}a, \frac{a}{\sqrt{6}}\varepsilon_4, \frac{a}{\sqrt{6}}\right),\ \mathbf{r}_{2'} = \left(\frac{\sqrt{3}}{2}a, -\frac{a}{2}, 0\right),\ \mathbf{r}_{2''} = \left(\frac{\sqrt{3}}{2}a, \frac{a}{2}, 0\right),$$

$$\mathbf{r}_3 = \left(\frac{a}{\sqrt{3}}, -\frac{a}{\sqrt{6}}\varepsilon_4, -\frac{a}{\sqrt{6}}\right),\ \mathbf{r}_4 = \left(\frac{a}{\sqrt{3}}, -\sqrt{\frac{2}{3}}a\varepsilon_4, \sqrt{\frac{2}{3}}a\right),\ \mathbf{r}_{5'} = \left(\frac{a}{2\sqrt{3}}, \frac{a}{2}\left(-1+\sqrt{\frac{2}{3}}\varepsilon_4\right), \frac{a}{\sqrt{6}}\right),$$

$$\mathbf{r}_{5''} = \left(\frac{a}{2\sqrt{3}}, \frac{a}{2}\left(1+\sqrt{\frac{2}{3}}\varepsilon_4\right), \frac{a}{\sqrt{6}}\right). \tag{6}$$

Deformation of ε_5 type shifts the coordinates in the z direction: $r_z = \left(r_z\right)_0 + \left(r_x\right)_0 \cdot \varepsilon_5$:

$$\mathbf{r}_1 = \left(\frac{2}{\sqrt{3}}a, 0, \frac{a}{\sqrt{6}} + \frac{2a}{\sqrt{3}}\varepsilon_5\right),\ \mathbf{r}_{2'} = \left(\frac{\sqrt{3}}{2}a, -\frac{a}{2}, \frac{\sqrt{3}}{2}a\varepsilon_5\right),\ \mathbf{r}_{2''} = \left(\frac{\sqrt{3}}{2}a, +\frac{a}{2}, \frac{\sqrt{3}}{2}a\varepsilon_5\right),$$

$$\mathbf{r}_3 = \left(\frac{a}{\sqrt{3}}, 0, -\frac{a}{\sqrt{6}} + \frac{a}{\sqrt{3}}\varepsilon_5\right),\ \mathbf{r}_4 = \left(\frac{a}{\sqrt{3}}, 0, +\sqrt{\frac{2}{3}}a + \frac{a}{\sqrt{3}}\varepsilon_5\right),$$

$$\mathbf{r}_{5'} = \left(\frac{a}{2\sqrt{3}}, -\frac{a}{2}, \frac{a}{\sqrt{6}} + \frac{a}{2\sqrt{3}}\varepsilon_5\right),\ \mathbf{r}_{5''} = \left(\frac{a}{2\sqrt{3}}, \frac{a}{2}, \frac{a}{\sqrt{6}} + \frac{a}{2\sqrt{3}}\varepsilon_5\right) \tag{7}$$

Deformation of ε_6 type shifts the coordinates in the y direction: $r_y = \left(r_y\right)_0 + \left(r_x\right)_0 \cdot \varepsilon_6$:

$$\mathbf{r}_1 = \left(\frac{2}{\sqrt{3}}a, \frac{2a}{\sqrt{3}}\varepsilon_6, \frac{a}{\sqrt{6}}\right),\ \mathbf{r}_{2'} = \left(\frac{\sqrt{3}}{2}a, \frac{a}{2}\left(-1+\sqrt{3}\varepsilon_6\right), 0\right),\ \mathbf{r}_{2''} = \left(\frac{\sqrt{3}}{2}a, \frac{a}{2}\left(1+\sqrt{3}\varepsilon_6\right), 0\right),$$

$$\mathbf{r}_3 = \left(\frac{a}{\sqrt{3}}, \frac{a}{\sqrt{3}}\varepsilon_6, -\frac{a}{\sqrt{6}}\right),\ \mathbf{r}_4 = \left(\frac{a}{\sqrt{3}}, \frac{a}{\sqrt{3}}\varepsilon_6, \sqrt{\frac{2}{3}}a\right),\ \mathbf{r}_{5'} = \left(\frac{a}{2\sqrt{3}}, \frac{a}{2}\left(-1+\frac{1}{\sqrt{3}}\varepsilon_6\right), \frac{a}{\sqrt{6}}\right),$$

$$\mathbf{r}_{5''} = \left(\frac{a}{2\sqrt{3}}, \frac{a}{2}\left(1+\frac{1}{\sqrt{3}}\varepsilon_6\right), \frac{a}{\sqrt{6}}\right). \tag{8}$$

3.3. Energy level shifts induced by the deformations

The elastic modulus in equation (1) is defined as follows (see, e.g., reference[10]):

$$\left(c_{\mathrm{JT}}^{\mathrm{T}}\right)_{ii} = -n\kappa T\left(\frac{\partial^2 \ln Z}{\partial \varepsilon_i{}^2}\right)_{\varepsilon=0}, \tag{9}$$

where the partition function Z takes into account the shifts of the (populated) energy levels ΔE_m produced by the deformations:

$$Z = \sum_m \exp\left(-\frac{\Delta E_m}{\kappa T}\right). \tag{10}$$

In the $T \otimes e$ JT problem at low temperatures, assuming that only one, the lowest vibronic state in the minima is populated, the shifts of the energy levels are defined by the linear vibronic coupling constant F_E, which has the meaning of the electron-deformation constant induced by the JTE, and the excess deformation induced by the ultrasound wave. According to the vibronic theory (see reference,[1] Ch. 4 and 5) the vibronic energy level in this problem are lowered by the JTE deformation in the minima of the APES by the amount of the JTE stabilization energy $E_{\mathrm{JT}}^{\mathrm{E}}$,

$$E_{\mathrm{JT}}^{\mathrm{E}} = \frac{F_{\mathrm{E}}^2}{2K_{\mathrm{E}}} = \frac{1}{2} K_{\mathrm{E}} Q_0^2 \ , \tag{11}$$

where K_{E} is the primary force constant characterizing the stiffness of the crystal without the vibronic coupling, Q_0 is the *e* type distortion at the point of the minimum of the APES, and we took into account that $Q_0 = F_{\mathrm{E}} / K_{\mathrm{E}}$. Now we take into account the additional distortion of the complex incurred under the ultrasonic wave. As mentioned above, the *e* type distortion of the JT center is equivalent to the tetragonal distortion of the crystal elongating the related cube edge Δb_m , where m number the minima of the APES. Figure 5 illustrates this situation (see also figures 2 and 4). It means that the distortion Q_0 under the wave deformation becomes $Q_0 + \Delta b_m$ resulting in the shift of the vibronic energy level position:

$$\Delta E_m = \frac{1}{2} K_E \left(Q_0 + \Delta b_m\right)^2 - \frac{1}{2} K_E Q_0^{\ 2} = F_E \Delta b_m + \frac{1}{2} K_E \left(\Delta b_m\right)^2 \approx F_E \Delta b_m \ , \tag{12}$$

where we ignored the quadratic deformations as compared with the linear ones.

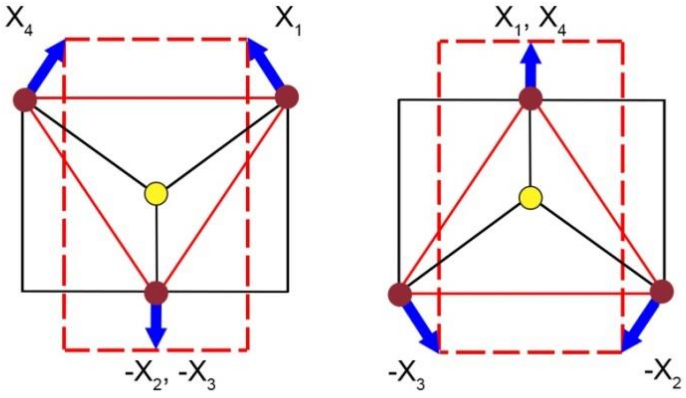

Figure 5. Direct and 90^0-rotated projection view of one of the two *e* type displacement of the tetrahedral environment of the Cr ion in the JT center, $Q_\vartheta = (1/2)\left(X_1 - X_2 - X_3 + X_4\right)$.[1] In the bulk this deformation is equivalent to elongation Δb of the edge of the related cube (see also figures 2 and 4).

A similar formula can be obtained for the shift of the vibronic energy levels ΔE_m of the $T \otimes t_2$ JT problem at low temperatures,

$$\Delta E_m \approx \frac{2}{\sqrt{3}} F_T \Delta d_m , \tag{13}$$

where Δd_m is the change in the related-cube diagonal produced by the ultrasonic wave, and F_T is the trigonal vibronic coupling constant. But in this case, in addition to ignoring the quadratic effect, we ignore also the initial tunneling splitting of the vibronic levels, assuming that they are small (there is no tunneling splitting in the $T \otimes e$ problem). The result of the calculations of the energy level shifts caused by the ultrasound deformations in the $T \otimes e$ and $T \otimes t_2$ JT problems are given in the tables 2, and 3, respectively.

Table 2. The energy level shifts under the deformations ε_i in the $T \otimes e$ JT problem.

	ΔE_1	ΔE_2	ΔE_3
ε_1	$F_E \frac{\sqrt{2}a}{3}\varepsilon_1$	$F_E \frac{a}{6\sqrt{2}}\varepsilon_1$	$F_E \frac{a}{6\sqrt{2}}\varepsilon_1$
ε_3	$F_E \frac{a}{3\sqrt{2}}\varepsilon_3$	$F_E \frac{a}{3\sqrt{2}}\varepsilon_3$	$F_E \frac{a}{3\sqrt{2}}\varepsilon_3$
ε_4	0	$-\frac{F_E a}{2\sqrt{3}}\varepsilon_4$	$\frac{F_E a}{2\sqrt{3}}\varepsilon_4$
ε_5	$-F_E \frac{a}{3}\varepsilon_5$	$F_E \frac{a}{6}\varepsilon_5$	$F_E \frac{a}{6}\varepsilon_5$
ε_6	0	$-F_E \frac{a}{2\sqrt{6}}\varepsilon_6$	$F_E \frac{a}{2\sqrt{6}}\varepsilon_6$

Table 3. The energy level shifts under the deformations ε_i in the $T \otimes t_2$ JT problem.

	ΔE_1	ΔE_2	ΔE_3	ΔE_4
ε_1	$F_T \frac{8\sqrt{2}a}{9}\varepsilon_1$	0	$F_T \frac{2\sqrt{2}a}{9}\varepsilon_1$	$F_T \frac{2\sqrt{2}a}{9}\varepsilon_1$
ε_3	$F_T \sqrt{2}a\varepsilon_3$	$F_T \frac{\sqrt{2}a}{9}\varepsilon_3$	$F_T \frac{\sqrt{2}a}{9}\varepsilon_3$	$F_T \frac{\sqrt{2}a}{9}\varepsilon_3$
ε_4	0	0	$-F_T \frac{2a}{3\sqrt{3}}\varepsilon_4$	$F_T \frac{2a}{3\sqrt{3}}\varepsilon_4$
ε_5	$F_T \frac{4a}{9}\varepsilon_5$	0	$-F_T \frac{2a}{9}\varepsilon_4$	$-F_T \frac{2a}{9}\varepsilon_4$
ε_6	0	0	$F_T \frac{\sqrt{2}a}{3\sqrt{3}}\varepsilon_6$	$-F_T \frac{\sqrt{2}a}{3\sqrt{3}}\varepsilon_6$

In case of the $T\otimes\left(e+t_2\right)$ JT problem, the minima of the APES are either tetragonal, and then the vibronic energy shifts follow equation (12), or trigonal with the shifts (13). In the very strong quadratic vibronic coupling approximation the minima of the APES in this case may become orthorhombic,[11,12] but this is a rather rare possibility. In this case ΔE_m are defined by a (strongly dependent on the specific system) combination of the two linear vibronic coupling constants F_{E} and F_{T} [1,11,12]. Using coordinates of orthorhombic extrema (see page 67 in reference[1]) and equations (12) and (13), we can derive expressions for the energy shifts produced by the ultrasonic modes in this case, as follows:

$$\left(\Delta E_{JT}^{O}\right)_1=\frac{1}{4}\left(-F_E\Delta b_1\right)+\frac{3}{4}\left(\frac{2}{\sqrt{3}}F_T\left(\Delta d_1+\Delta d_2\right)\right), \tag{14}$$

$$\left(\Delta E_{JT}^{O}\right)_2=\frac{1}{4}\left(-F_E\Delta b_1\right)+\frac{3}{4}\left(\frac{2}{\sqrt{3}}F_T\left(\Delta d_3+\Delta d_4\right)\right), \tag{15}$$

$$\left(\Delta E_{JT}^{O}\right)_3=\frac{1}{4}\left(-F_E\Delta b_2\right)+\frac{3}{4}\left(\frac{2}{\sqrt{3}}F_T\left(\Delta d_1+\Delta d_3\right)\right), \tag{16}$$

$$\left(\Delta E_{JT}^{O}\right)_4=\frac{1}{4}\left(-F_E\Delta b_2\right)+\frac{3}{4}\left(\frac{2}{\sqrt{3}}F_T\left(\Delta d_2+\Delta d_4\right)\right), \tag{17}$$

$$\left(\Delta E_{JT}^{O}\right)_5=\frac{1}{4}\left(-F_E\Delta b_3\right)+\frac{3}{4}\left(\frac{2}{\sqrt{3}}F_T\left(\Delta d_1+\Delta d_4\right)\right), \tag{18}$$

$$\left(\Delta E_{JT}^{O}\right)_6=\frac{1}{4}\left(-F_E\Delta b_3\right)+\frac{3}{4}\left(\frac{2}{\sqrt{3}}F_T\left(\Delta d_2+\Delta d_3\right)\right), \tag{19}$$

For the mode related to c_{33} we have:

$$\left(\Delta E_{JT}^{O}\right)_1=\left(\Delta E_{JT}^{O}\right)_3=\left(\Delta E_{JT}^{O}\right)_5=\left(-\frac{F_E}{12\sqrt{2}}+\frac{5F_T}{3\sqrt{2}}\right)a\varepsilon_3, \tag{20}$$

$$\left(\Delta E_{JT}^{O}\right)_2=\left(\Delta E_{JT}^{O}\right)_4=\left(\Delta E_{JT}^{O}\right)_6=\left(-\frac{F_E}{12\sqrt{2}}+\frac{F_T}{3\sqrt{2}}\right)a\varepsilon_3. \tag{21}$$

3.4. Relaxation in the JT subsystem

The results presented in tables 2, and 3 show that, in general, the deformation produced by the ultrasonic wave shifts the vibronic levels in different ways, resulting in a non-equilibrium state of the JT center with possible relaxations (leading to dissipation of the wave energy), as illustrated in figure 6(a). Notably, in the case of the $T\otimes e$ problem all the three energy levels are shifted identically under the ε_3 type deformation (figure 6(a)), leaving the three minima of the JT center in thermal equilibrium. This follows directly from the calculation of the $\left(c_{\mathrm{JT}}^{\mathrm{T}}\right)_{33}$ modulus using equations (9) and (10) with the $\Delta E_m\left(\varepsilon_3\right)$ values from table 2; for the $T\otimes e$ JT problem the calculation yields

$\left(c_{\mathrm{JT}}^{\mathrm{T}}\right)_{33}=0$. Consequently, for this case the ultrasound relaxation rate $\alpha_3=0$, whereas for all the other deformation types $\left(c_{\mathrm{JT}}^{\mathrm{T}}\right)_{ii}\neq 0$ and $\alpha_i\neq 0$. Three identical shifts of three levels occur under the ε_3 type deformation also in the $T\otimes\left(e+t_2\right)$ JT problem with orthorhombic minima (equation (20) and (21)), but in this case there are other three levels exhibit different shifts and a nonzero relaxation may takes place (figure 6(c)).

This result explains directly the origin of the zero anomalies in the temperature dependence of the attenuation of modulus c_{33} ultrasound, and its nonzero value for all the other moduli (figure 3), as well as the realization of the $T\otimes e$ JTE in the Cr^{2+} centers of the impurity crystal CdSe:Cr^{2+}. It supports also the new approach to the problem of ultrasound investigation of structure and properties of JT impurity centers in non-cubic crystals, introduced in this paper. Note, however, that the local high symmetry coordination of an impurity may be significantly violated by the lower symmetry host crystal, thus destroying or modifying the JTE. For example, in the layered perovskite K_2ZnF_4: Cu^{2+} crystal the complex CuF_6 is practically a regular octahedron, but the anisotropic field of its environment suppresses the JTE. [13]

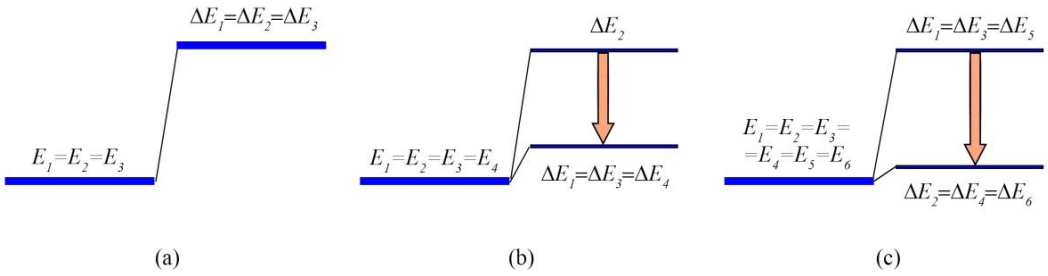

Figure 6. Scheme of the shifts of the energy levels ΔE_i under the deformations of ε_3 type in the $T\otimes e$ JT problem (a), $T\otimes t_2$ problem (b), and at quadratic $T\otimes\left(e+t_2\right)$ problem (c). In the $T\otimes e$ case all the three vibronic energy level shift identically, hence no JT center induced relaxation of c_{33} elastic modulus is possible in this case.

4. Conclusion

In a more general view, the main result of this paper is in the developed new procedure that allows to rationalize the outcome of ultrasonic experiments in terms of the local distortions in JTE centers of impurity crystals with non-cubic bulk symmetry. In such crystals, their symmetry axes do not necessarily coincide with the symmetries of the JT active modes, leading to a controversy in the attempt to interpret the experimental results with the methodology worked out for cubic crystals.

In the newly worked out method we find direct relations between ultrasonic deformations (atomic displacements by the sound wave) and JT modes in all the possible JTE problems, showing how to do it using the wurtzite crystal CdSe:Cr^{2+} as a working example. In this case the Cr^{2+} JT center has an electronic ground state T term in a tetrahedral environment, but the bulk symmetry of the crystal is hexagonal, and the cube associated with the tetrahedral JT complex is inclined with respect to hexagonal axis. Therefore, the normal mode of ultrasonic deformations produces distortions of the JT complex that are linear combinations of the JTE modes. The example-case of CdSe:Cr^{2+} proved to be very favorable because its JTE induced relaxation anomalies are absent only for one mode ε_3, for which the theory yields identical (uniform) shifts of all the vibronic energy levels (and hence no relaxation) in the case of the $T\otimes e$ JT problem only. In this situation we revealed the kind of JTE that takes place in the system under consideration (and hence all the other related properties) in a qualitative way, by observing that there is no JT induced relaxations of the c_{33} ultrasonic wave. In

more complicated cases the $\left(c_{\mathrm{JT}}^{\mathrm{T}}\right)_{ii}$ moduli should be calculated using the worked out procedures, reported in this paper.

Acknowledgment
This research work was carried out within the Russian state assignment No.AAAA-A18-118020190098-5. We acknowledge the support from the HLD at HZDR, member of the European Magnetic Field Laboratory (EMFL), from Russian Foundation for Basic Research (project 18-02-00332 a), and from UrFU Center of Excellence "Radiation and Nuclear Technologies" (Competitiveness Enhancement Program). N.S.A. thanks the Foundation for the Advancement of Theoretical Physics and Mathematics "BASIS" (Russia).

Appendix
To justify the statement about the relaxation origin of the ultrasound attenuation anomalies one has (i) to measure the temperature dependences of attenuation α for at least two frequencies of the ultrasound, ω and Ω (α_ω and α_Ω), (ii) with the data obtained with one of the frequencies, to evaluate the temperature dependence of the relaxation time τ_ω, and (iii) since the relaxation time is assumed to be frequency independent, to reveal the temperature dependence of the attenuation $\alpha_\Omega\left(T,\tau_\omega\right)$ taking into account the obtained relaxation time τ_ω and using equation (1). If the measured and calculated attenuations coincide with the experimental accuracy, equation (1) describes the mechanism of attenuation correctly, and the nature of the wave's energy dissipation is relaxation.

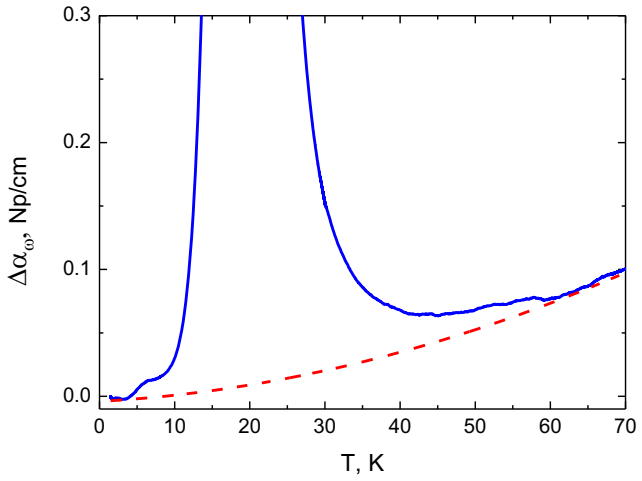

Figure A1. Temperature dependence of attenuation of the mode related to the c_{55} modulus (solid line, $\omega/2\pi = 29.6$ MHz) and the background attenuation (dashed line) defined as $\alpha_{\mathrm{b}} = -0.004 + 0.0033\cdot T + 0.000016\cdot T^2$.

Extraction of the relaxation time from the experimental data on ultrasonic attenuation consists of (i) determination of relaxation attenuation caused by the JT subsystem $\alpha_{\mathrm{rel}}\left(T\right) = \alpha\left(T\right) - \alpha_{\mathrm{b}}\left(T\right)$, where $\alpha\left(T\right)$ is total attenuation and $\alpha_{\mathrm{b}}\left(T\right)$ is the background attenuation determined by all the sources except the JT one, and (ii) calculation of the temperature dependence of the relaxation time with the use of the following expression (see, e.g., reference [2]):

$$\tau_{\omega}(T)=\frac{1}{\omega}\left\{\frac{\alpha_{\mathrm{rel}}(T_1)\cdot T_1}{\alpha_{\mathrm{rel}}(T)\cdot T}\pm\left[\left(\frac{\alpha_{\mathrm{rel}}(T_1)\cdot T_1}{\alpha_{\mathrm{rel}}(T)\cdot T}\right)^2-1\right]^{1/2}\right\}, \tag{A1}$$

where T_1 corresponds to the condition $\omega\tau(T_1)=1$. Figure A1 shows the result of the simulation of $\alpha_{\mathrm{b}}(T)$ assuming that the background attenuation is a smooth function, which coincides approximately with the measured attenuation at low and high temperatures outside the peak position.

The result of the calculations with the use of equation (2) and the obtained function $\alpha_{\mathrm{rel}}(T)$ is shown in figure A2.

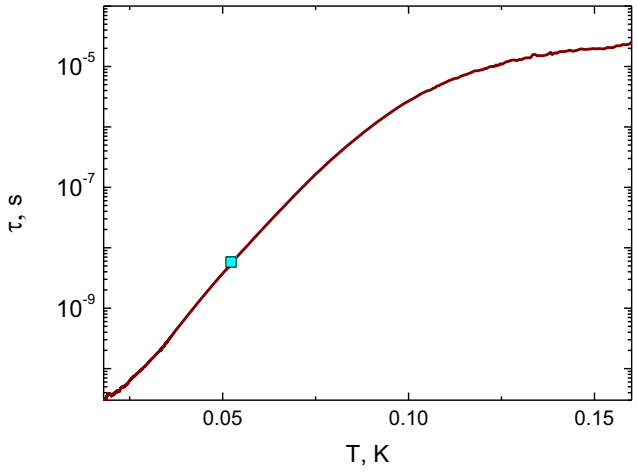

Figure A2. Temperature dependence of relaxation time obtained for the normal mode related to the c_{55} modulus at $\omega/2\pi=29.6$ MHz. The square symbol defines the condition $\omega\tau(T_1)=1$ at this frequency.

The relaxation attenuation given by equation (1) can be expressed in terms of τ and the experimental parameters as follows: [5]

$$\alpha_{\mathrm{rel}}(\omega,T)=2\frac{\alpha_{\mathrm{rel}}(\omega,T_1)\cdot T_1}{T}\frac{\omega\tau}{1+(\omega\tau)^2}\ . \tag{A2}$$

The attenuation at any other frequency can be determined using equation (3):

$$\alpha_{\mathrm{rel}}(\Omega,T)=2\frac{\Omega}{\omega}\frac{\alpha_{\mathrm{rel}}(\omega,T_1)\cdot T_1}{T}\frac{\Omega\tau}{1+(\Omega\tau)^2}\ . \tag{A3}$$

Important comment: T_1 in both equations (A2) and (A3) is the same, i.e., it corresponds to the condition $\omega\tau(T_1)=1$, and it is defined from the experimental data of $\alpha_{\mathrm{rel}}(\omega,T)$. The results of simulation with use of equation (A3) are given in figure A3. The agreement of the calculated attenuation and measured one at 55.4 MHz may be considered as being satisfactory: the measurements at 29.6 and 55.4 MHz require to change of the transducers, and it is very difficult to mount them

exactly at the same place. Therefore, the inhomogeneity of the specimen regarding the concentration of the dopant influences the results.

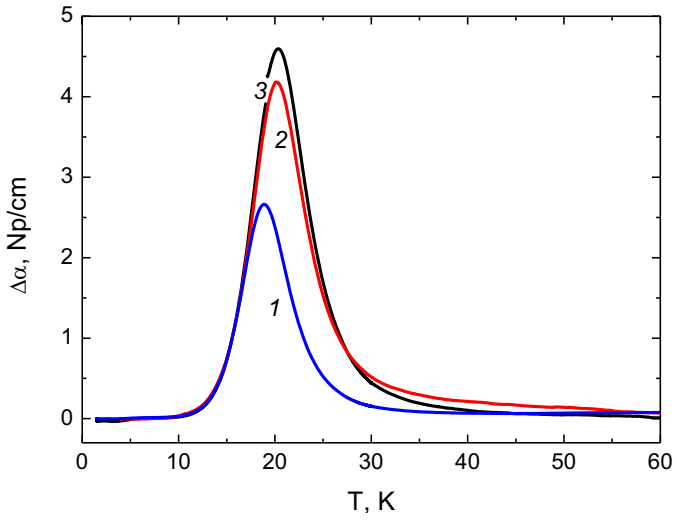

Figure A3. Temperature dependence of the attenuation of the mode related to the c_{55} modulus obtained at $\omega/2\pi = 29.6$ MHz (curve 1), $\Omega/2\pi = 55.4$ MHz (curve 2), and calculated with the use of equation (A3) (curve 3).

References

[1] Bersuker I B 2006 *The Jahn-Teller Effect* (Cambridge: Cambridge University Press)
[2] Gudkov V V and Bersuker I B 2012 Experimental Evaluation of the Jahn-Teller Effect Parameters by Means of Ultrasonic Measurements. Application to Impurity Centers in Crystals in *Vibronic Interaction and the Jahn-Teller Effect* eds M Atanasov, C Daul, P L Treggenna-Piggot (Heidelberg: Springer) pp 143-161
[3] Averkiev N S, Bersuker I B, Gudkov V V, Zhevstovskikh I V, Baryshnikov K A, Sarychev M N, Zherlitsyn S, Yasin S and Korostelin Yu V 2017 *Phys.Rev.B* **96** 094431
[4] Zhevstovskikh I V, Bersuker I B, Gudkov V V, Averkiev N S, Sarychev M N, Zherlitsyn S, Yasin Sh, Shakurov G S, Ulanov V A and Surikov V T 2016 *J. Appl. Phys.***119** 225108
[5] Averkiev N S, Bersuker I B, Gudkov V V, Zhevstovskikh I V, Sarychev M N, Zherlitsyn S, Yasin S, Shakurov G S, Ulanov V A, Surikov V T 2017 *J. Phys. Soc. Jpn*. **86** 114604
[6] Averkiev N S, Bersuker I B, Gudkov V V , Baryshnikov K A, Colibaba G V, Zhevstovskikh I V, Mayakin V Yu, Monakhov A M, Nedeoglo D D, Sarychev M N, and Surikov V T 2014 *Phys. Status Solidi B* **251** 1590
[7] Korostelin Yu V and Kozlovsky V I 2004 *J. Alloys Comp.* **371** 25
[8] Luthi B 2005 *Physical Acoustics in the Solid State* (Springer, Berlin)
[9] Gudkov V V and Gavenda J D 2000 *Magnetoacoustic Polarization Phenomena in Solids* (Springer-Verlag, New York, Berlin, Heidelberg) pp 27-31
[10] Sturge M D 1967 The Jahn-Teller Effect in Solids in *Solid State Physics* eds Seitz F, Turnbull D, Ehrenreich H (Academic Press, New York and London) volume 20 pp 91-211
[11] Bersuker I B, Polinger V Z 1974 *Zh. Eksp. Teor. Fiz.* **66** 2078 [Sov. Phys. *JETP* **39** 1023]
[12] Bersuker I B, Polinger V Z *Vibronic Interaction in Molecules and Crystals* 1989 (Springer, Heidelberg)
[13] Aramburu J A, Garsia-Lastra J M, Garsia-Fernándes P, Barriuso M T, and Moreno M 2013 *Inorg.Chem.* **52** 6923